



Contents lists available at ScienceDirect

# Spectrochimica Acta Part A: Molecular and Biomolecular Spectroscopy

journal homepage: [www.journals.elsevier.com/spectrochimica-acta-part-a-molecular-and-biomolecular-spectroscopy](http://www.journals.elsevier.com/spectrochimica-acta-part-a-molecular-and-biomolecular-spectroscopy)

## A study of O—H...O hydrogen bonds along various isolines in 2-ethyl-1-hexanol. Temperature or pressure - which parameter controls their behavior?

Barbara Hachuła<sup>a,\*</sup>, Ewa Kamińska<sup>b</sup>, Kajetan Koperwas<sup>c</sup>, Roman Wrzalik<sup>c</sup>, Karolina Jurkiewicz<sup>c</sup>, Magdalena Tarnacka<sup>c</sup>, Demetrio Scelta<sup>d,e</sup>, Samuele Fanetti<sup>d,e</sup>, Sebastian Pawlus<sup>c,\*</sup>, Marian Paluch<sup>c</sup>, Kamil Kamiński<sup>c</sup>

<sup>a</sup> Institute of Chemistry, Faculty of Science and Technology, University of Silesia in Katowice, Szkolna 9, 40-006 Katowice, Poland

<sup>b</sup> Department of Pharmacognosy and Phytochemistry, Faculty of Pharmaceutical Sciences in Sosnowiec, Medical University of Silesia in Katowice, Jagiellońska 4, 41-200 Sosnowiec, Poland

<sup>c</sup> Institute of Physics, Faculty of Science and Technology, University of Silesia in Katowice, 75 Pułku Piechoty 1, 41-500 Chorzów, Poland

<sup>d</sup> LENS, European Laboratory for Non-linear Spectroscopy, Via N. Carrara 1, I-50019 Sesto Fiorentino, Firenze, Italy

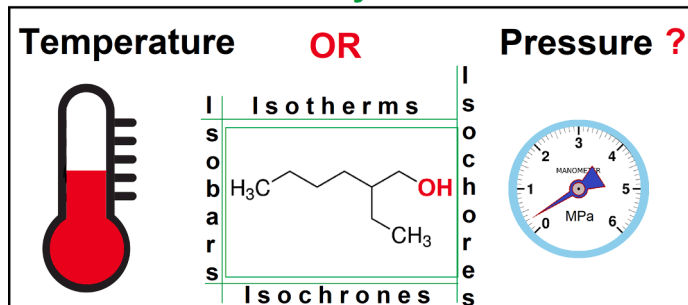
<sup>e</sup> ICCOM-CNR, Institute of Chemistry of OrganoMetallic Compounds, National Research Council of Italy, Via Madonna del Piano 10, I-50019 Sesto Fiorentino, Firenze, Italy

### HIGHLIGHTS

- The unique high-pressure infrared, dielectric, and volumetric data were analyzed.
- $T$  and  $p$  dependence of H-bonding energy along various isolines was studied.
- A phase diagram of 2E1H, identifying isolines in the  $T$ - $p$  plane, was constructed.
- $T$  controls the intramolecular dynamics of O—H units in 2E1H.
- The impact of density fluctuation grows with increasing  $T$  and weakening of HBs.

### GRAPHICAL ABSTRACT

## The intramolecular dynamics of OH units



### ARTICLE INFO

**Keywords:**  
Hydrogen bond  
Temperature  
Pressure  
Isolines  
Intramolecular dynamics

### ABSTRACT

The nature of H-bonding interactions is still far from being understood despite intense experimental and theoretical studies on this subject carried out by the leading research centers. In this paper, by a combination of unique high-pressure infrared, dielectric and volumetric data, the intramolecular dynamics of hydroxyl moieties (which provides direct information about H-bonds) was studied along various isolines, i.e., isotherms, isobars, isochrones, and isochores, in a simple monohydroxy alcohol (2-ethyl-1-hexanol). This allowed us to discover that the temperature controls the intermolecular hydrogen bonds, which then affect the intramolecular dynamics of O—H units. Although the role of density fluctuations gets stronger as temperature rises. We also demonstrated a clear connection between the intra- and intermolecular dynamics of the associating liquid at high pressure. The

\* Corresponding authors.

E-mail addresses: [barbara.hachula@us.edu.pl](mailto:barbara.hachula@us.edu.pl) (B. Hachuła), [sebastian.pawlus@us.edu.pl](mailto:sebastian.pawlus@us.edu.pl) (S. Pawlus).

<https://doi.org/10.1016/j.saa.2022.121726>

Received 23 May 2022; Received in revised form 18 July 2022; Accepted 5 August 2022

Available online 8 August 2022

1386-1425/© 2022 The Author(s). Published by Elsevier B.V. This is an open access article under the CC BY license (<http://creativecommons.org/licenses/by/4.0/>).

data reported herein open a new perspective to explore this important aspect of the glass transition phenomenon and understand H-bonding interactions at varying thermodynamic conditions.

## 1. Introduction

Pressure ( $p$ ) is a fundamental thermodynamic variable that affects the distances between molecules (molecular packing), depth, and shape of the potential well describing intermolecular interactions [1–3]. Consequently, it has a tremendous impact on the physics and chemistry of the studied matter. As an example, one can mention that previous studies performed at varying thermodynamic conditions demonstrated that it is possible to shorten reaction times and synthesize materials of unique properties or geometry not attainable at ambient pressure [4–5]. What is more, the experiments allowed inducing quite an extraordinary variation in physical features of the compressed matter. In this context, it is worth reminding of the most spectacular ones, such as gas metalization, the transition from insulator to superconductor, ionization of water, or ammonia that occur at high compression [6–8].

Furthermore, the studies at elevated pressure were the key to better understanding the essence of H-bonds (HBs) – one of the most fundamental and crucial electrostatic interactions occurring in nature. Briefly, one can recall that this type of molecular interactions i) underlies all-important processes undergoing in the living organisms, as well as the self-assembly phenomenon, ii) determines the biological activity of proteins, or iii) the peculiar behavior of water and other associating liquids. Herein, it should be added that extensive high-pressure (HP) studies on the H-bonded liquids clearly indicated that their dynamical and thermodynamical properties, such as pressure evolution of the relaxation times, diffusion, pressure coefficient of the glass transition temperature, activation volume, bulk moduli, and thermal expansion coefficient, are much different with respect to the van der Waals systems [9–12]. What is more, it was experimentally observed that the thermodynamic scaling (TS) – a hotly debated concept that links dynamical properties (relaxation times) with the exponent describing intermolecular repulsion between molecules, is usually not satisfied for liquids forming HBs. However, it is not a rule, and the TS seems to depend on the strength of H-bonds, variation in the architecture of nanoassociates, range of  $p$ , etc. A good illustration of a deviation from the TS rule is 2-ethyl-1-hexanol (2E1H) – a simple monohydroxy alcohol, for which the scaling exponent is not constant above 500 MPa [13–15]. Interestingly, this extraordinary behavior was linked with the change of the H-bonding pattern in the sample. Nevertheless, it should be emphasized that the mentioned example and others described above are devoted to investigating the behavior of associated liquids at high  $p$ , not HBs themselves. Over recent years, using indirect experimental methods was the most common way and serious drawback of probing HBs under high  $p$ . As a consequence of that, there are different points of view on the impact of high compression on the strength and population of this kind of bonds at different temperature and pressure conditions. Based on dielectric data, it was postulated that HBs are being broken, and their population decreases with the increase in  $p$  [16–18]. On the other hand, the simulation data obtained for various systems indicated no effect of pressure or the enhancement of these interactions with compression [19–20]. Finally, Fourier-Transform Infrared (FTIR) and Raman studies revealed a monotonic increase in the strength of HBs with  $p$  [21–22]. In fact, the former technique is the most sensitive and fully dedicated to probing the properties of H-bonded associates at varying thermodynamic conditions. It is worth emphasizing that the length, as well as the angle between the proton donor (X-H) and acceptor (Y) groups, influence the frequency of the stretching vibration of the hydroxyl units ( $\nu_{\text{O-H}}$ ) and the shape of the related band [23]. Therefore, any variation in the spectroscopic parameters, namely frequency, the full width at half maximum (FWHM), or the integral intensity of the  $\nu_{\text{X-H}}$  band, may provide unique information on the real effect of compression on the

behavior of HBs. Nevertheless, due to the high intensity of the mentioned band in FTIR experiments under high pressure, performed usually in diamond anvil cells (DAC) [24–25], determination of the credible parameters describing these specific interactions is quite difficult.

In this paper, we applied the vibrational spectroscopy technique combined with the DAC to measure FTIR spectra of 2E1H at high  $p$ . To obtain samples of uniform thickness and absorbance value, DAC was filled with the tested alcohol and very thin polyethylene foil. The collected data yielded fundamental information about the impact of pressure on HBs. Furthermore, by combining dielectric and volume data with the ones obtained from FTIR investigations, we were able to make credible conclusions about the behavior of H-bonding interactions along different isolines, namely isotherms (temperature,  $T=\text{const.}$ ), isobars ( $p = \text{const.}$ ), isochrones (relaxation times,  $\tau_\alpha=\text{const.}$ ) and isochores (volume,  $V=\text{const.}$ ). Finally, for the first time, we evaluated the effect of density and temperature on the energy/strength of HBs.

## 2. Materials and methods

2-ethyl-1-hexanol (2E1H) was purchased from Sigma-Aldrich (purity > 99 %). Before use, the alcohol was dried under a stream of liquid nitrogen. The chemical structure of the studied compound is presented in Scheme 1.

### 2.1. High-pressure (HP) Fourier Transform infrared (FTIR) spectroscopy

FTIR absorption spectra were recorded using a Bruker-IFS 120 HR spectrometer suitably modified for experiments in DAC, with an instrumental resolution set to  $1 \text{ cm}^{-1}$  [26]. The sample pressure was measured by the ruby fluorescence method using a few mW of a 532 nm laser line from a doubled Nd:YAG laser source. 2E1H was loaded into a membrane diamond anvil cell (MDAC) equipped with type IIa synthetic diamonds from Almax easyLab Inc., together with a small ruby chip as a pressure gauge. A thin pellet of polyethylene was used to reduce the sample thickness and to have an O–H absorbance from 0.1 to 1. All samples were laterally contained by steel gaskets, drilled to have an initial sample diameter of 150  $\mu\text{m}$  and a thickness of about 50  $\mu\text{m}$ . High-temperature runs were carried out using resistive heaters, and the temperature was measured by means of a K-type thermocouple with an accuracy of  $\pm 0.1 \text{ K}$ .

It should be added that the analysis of spectral parameters (the peak position, FWHM, integrated intensity) for the bands measured at HP was a challenging task due to the interference fringes disturbing the data. This well-known and common effect occurring in the HP experiments results from multiple internal reflections inside the film with two nearly parallel surfaces leading to signatures of constructive and destructive interference. For this reason, the O–H peak positions were determined using the Fityk software (a data processing and nonlinear curve fitting program; version: 1.3.1.; url: <https://fityk.nieto.pl/>) by applying VoigtA peak profile functions adjusting the intensity and the width of the fitting curves [27]. It should also be noted that the band component analysis of the C–H stretching region, occurring at ca.  $3050\text{--}2700 \text{ cm}^{-1}$ , was excluded from the deconvolution of the O–H band due to the saturation of C–H bands. Moreover, this spectral region was strongly disturbed by absorption signals originating from the polyethylene spacers used to maintain a reliable absorbance value of the  $\nu_{\text{O-H}}$  band. Additionally, the fitting of poorly resolved and broad O–H bands with saturated components of C–H bands led to a large error, only worsening the final deconvolution result. One can stress that the sinusoidal background was determined from the particular fringes observed in each IR spectrum

individually and then was fitted to the measured data in order to facilitate the interpretation of the IR spectra without losing any spectral information. The experimental error for the band position in the HP FTIR spectra was estimated to be ca.  $\pm 5 \text{ cm}^{-1}$ , although for higher  $p$  ( $>3 \text{ GPa}$ ), it was ca.  $\pm 10 \text{ cm}^{-1}$  since the O—H band profile overlapped the C—H band region with increasing compression. Illustrative plots and details for the fitted spectra are shown in [Figure S1](#) in the [Supplementary Material](#) (SM).

## 2.2. Fourier Transform infrared (FTIR) spectroscopy

FTIR spectra measurements were also performed at atmospheric pressure in the temperature range 123–293 K using a Nicolet iS50 FTIR spectrometer (Thermo Scientific) with a Linkam THMS 600 heating/cooling stage (Linkam Scientific Instruments Ltd., Surrey, U.K.) mounted inside the sample stage of FTIR spectrometer. A sample of the studied alcohol was placed between two  $\text{CaF}_2$  windows, separated by a 15  $\mu\text{m}$  thick spacer, which ensured the uniform thickness of the sample and warranted the constant geometry of the system. The spectra were recorded in the range of 4000–400  $\text{cm}^{-1}$  at a resolution of 4  $\text{cm}^{-1}$ . For every spectrum, 16 scans were averaged. The temperature stabilization accuracy was equal to  $\pm 0.1 \text{ K}$ .

## 3. Results and discussion

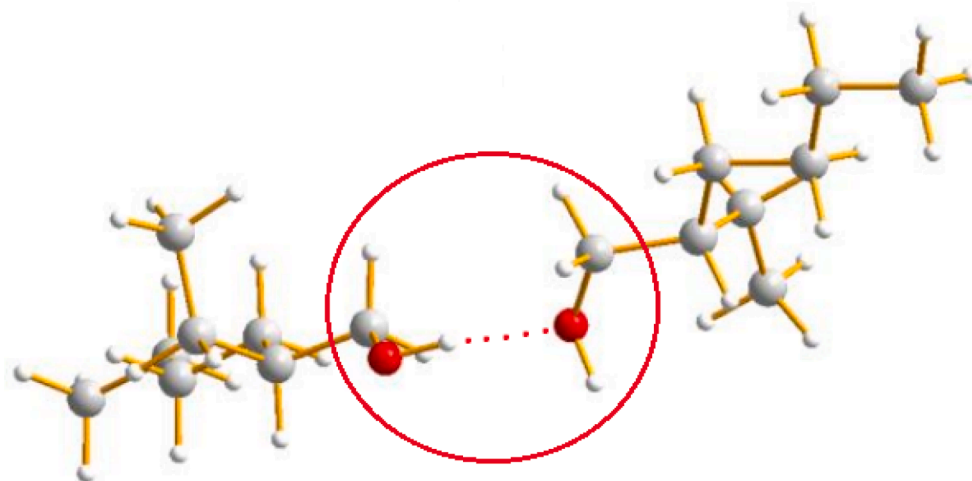
Despite the universal nature and ubiquity of HBs, so far, it has not been experimentally shown which thermodynamic parameter (temperature or pressure) has the most significant impact on their dynamics, pattern, and strength. Furthermore, it was not proven if there is any connection between the behavior of HBs and dynamics of associating liquids - an assumption made a priori by leading research groups. To gain an insight into these fundamental problems, we have carried out HP FTIR measurements on 2E1H, model alcohol, for which dielectric as well as volumetric data obtained at varying thermodynamic conditions are available in the literature [15,28]. IR spectra of 2E1H were collected upon compression runs up to  $p \sim 6 \text{ GPa}$  at four different  $T = 293, 308, 323, \text{ and } 348 \text{ K}$ . A separate IR experiment was performed at ambient pressure as a reference to track the changes in the behavior of HBs as a function of  $T$ . Herein, it must be stressed that to avoid the saturation effect of the stretching vibration of hydroxyl units at elevated  $p$ , a very thin polyethylene foil has been introduced between diamonds in an anvil cell. As a consequence, the dynamics and the spectral parameters originating from the vibrations of C—H units were highly affected by those coming from polyethylene. Therefore, this spectral range was

excluded from further analysis. What is more, the disturbance of the C—H bands also had a negative effect on the deconvolution of the  $\nu_{\text{O—H}}$  bands, as this absorption signal moved towards the C—H bands with increasing pressure. Another problem was the interference, which introduced a disturbance in the shape (the subtle structure) of the  $\nu_{\text{O—H}}$  band, influencing its spectral parameters (the peak position, FWHM, and integrated intensity). Data analysis revealed that the O—H band frequency is the least affected parameter due to interference and saturation effects. Hence, the evolution of this parameter as a function of varying thermodynamic conditions will be analyzed in more detail in this paper.

The temperature and pressure evolution of the IR spectra in the region of 3600–2500  $\text{cm}^{-1}$  is shown in [Figure 1](#) and [Figure S2](#) in the SM file. As can be seen, there is a broad absorption signal between 3600 and 3050  $\text{cm}^{-1}$  assigned to the stretching vibration of the O—H group, whereas the lower frequency band (3050–2700  $\text{cm}^{-1}$ ) corresponds to the C—H stretching vibrations. As mentioned above, the observed C—H bands were not taken for further analysis due to the saturation effect and overlapping with the vibrations originating from the polyethylene spacers.

At first, we analyzed the IR spectra measured during isobaric cooling. As shown in [Figure 1\(a\)](#), the stretching frequencies of the covalent O—H bonds are red-shifted (shifted to lower wavenumbers) with decreasing  $T$  due to the elongation of the O—H bond lengths (the strengthening of the H-bond interactions). This spectral modification, connected with a change in the X-H peak position of the H-bond donor molecule (where X is either O, Cl, C, N, or F), accompanying different external factors, i.e.,  $T$  or  $p$ , is an indicator of the strength of HBs. It is a well-known correlation that the larger the red-shift of the X-H band position, the stronger the hydrogen bond [29]. It should be mentioned that the high-precision *ab initio* methods of calculations applied recently on water dimer showed that the H-bond (H...O) becomes weaker with the contraction of H-bond length and O...O distance, which is attributed to the exchange repulsion of electrons [30–32].

Next, the effect of isothermal compression on the position of the band was considered. As can be observed in [Figure 1\(b\)](#), with increasing pressure, the  $\nu_{\text{O—H}}$  signal red-shifts and shows the monotonic change in the frequency with no discontinuities or changes in slope indicative of a phase change or crystallization. An analogous spectroscopic effect of lowering the frequency of the O—H band with the compression was observed for other IR spectra recorded as a function of  $p$  at 308, 323, and 348 K (see [Figure S2](#) in the SM file). Thus, the studied alcohol exhibits a typical pressure-induced behavior, i.e., the red-shift of the IR active O—H vibration with increasing pressure suggesting the strengthening of intermolecular HBs. A similar scenario was detected in



**Scheme 1.** The scheme of chemical structure of the H-bonded 2E1H under investigation.

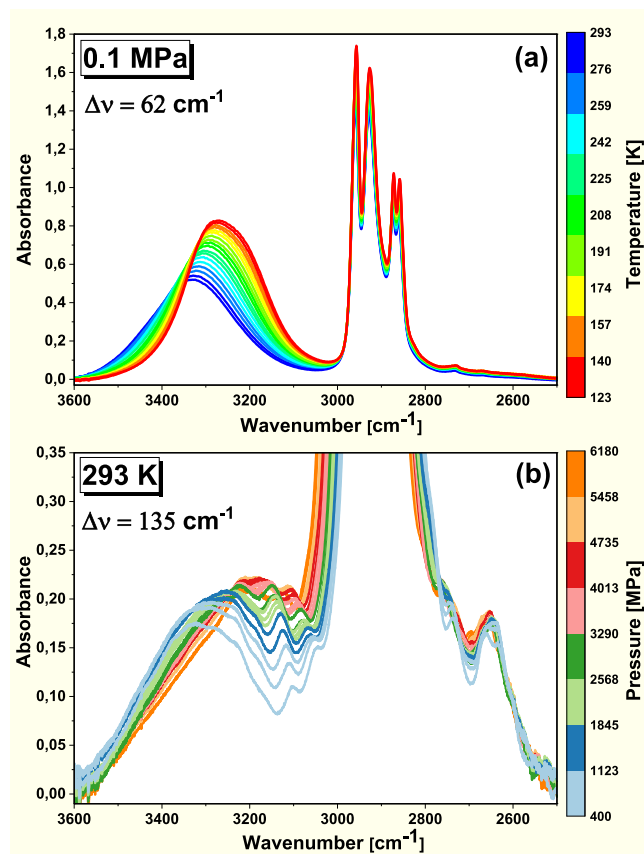


Fig. 1. FTIR spectra of 2E1H measured at (a)  $T = 293\text{--}123\text{ K}$  and  $p = 0.1\text{ MPa}$  and b)  $T = 293\text{ K}$  and  $p = 400\text{--}6170\text{ MPa}$  in the frequency region of  $3600\text{--}2500\text{ cm}^{-1}$ .

previous HP studies on methanol, ethanol, or ethylene glycol [22,33].

At first glance, one can see that the pressure had a greater effect on the position of the O—H band than temperature (Figure 1). The O—H peak frequency for the temperature-dependent IR spectra moved to the red regime by  $62\text{ cm}^{-1}$  (from  $293$  to  $123\text{ K}$ ) compared with the  $135\text{ cm}^{-1}$  shift obtained during the isothermal compression at  $293\text{ K}$  (from  $0.1$  to  $6170\text{ MPa}$ ) (for higher temperatures:  $\Delta\nu = 121\text{ cm}^{-1}/6140\text{ MPa}$  at  $308\text{ K}$ ;  $\Delta\nu = 166\text{ cm}^{-1}/6130\text{ MPa}$  at  $323\text{ K}$ ;  $\Delta\nu = 145\text{ cm}^{-1}/6290\text{ MPa}$  at  $348\text{ K}$ ). The much longer elongation of the O—H bond for an isobar compared to that of an isotherm indicates stronger H-bonding interactions occurring at high  $p$  than at  $123\text{ K}$ . This experimental finding suggests that isothermal compression (density) has a greater effect on the H-bond dynamics than isobaric cooling (combined effect of temperature and density fluctuations). However, this finding may be apparent since it is very difficult to compare directly pressurization effects (density packing) with a thermal variation. Hence to gain deeper insight into this problem, further analysis was performed.

Considering dielectric and volumetric data measured for 2E1H at various thermodynamic conditions (given in Refs. [15,28]), we decided to take a unique opportunity to monitor the behavior of H-bonding interactions along different isolines, namely isotherms ( $T = \text{const}$ ), isobars ( $p = \text{const}$ ), isochrones ( $\tau_\alpha = \text{const}$ ) and isochores ( $V = \text{const}$ ). Representative FTIR spectra at the following constant condition of (a) temperature, (b) specific volume ( $V_s = 0.88\text{ cm}^3\cdot\text{g}^{-1}$ ) and (c) relaxation times (viscosity) are shown in Figure 2. To determine the values of  $V$  for the given  $T$  and  $p$  conditions the Tait equation of state was used [15]:

$$V_s(T, p) = V_0 \exp(a_0 T) \left\{ 1 - C \ln \left[ 1 + \frac{p}{b_0 \exp(-b_1 T)} \right] \right\} \quad (1)$$

where:  $V_0 = 1.1729 \pm 10^{-4}\text{ cm}^3\cdot\text{g}^{-1}$ ,  $a_0 = (8.873 \pm 0.008) \cdot 10^{-4}\text{ C}^{-1}$

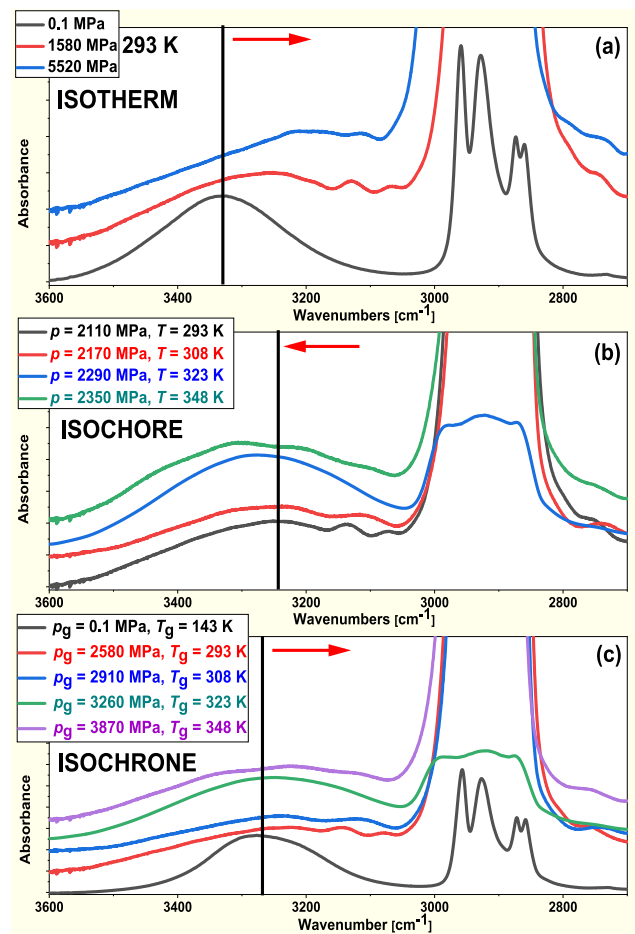


Fig. 2. FTIR spectra of 2E1H in the frequency region of  $3600\text{--}2600\text{ cm}^{-1}$  obtained after the deconvolution process, using sinusoidal and VoigtA formulas, at (a)  $293\text{ K}$  as a function of pressure, (b) constant specific volume ( $V_s = 0.88\text{ cm}^3\cdot\text{g}^{-1}$ ), and (c) at isochronal conditions determined from the pressure dependences of the glass transition temperature for the alcohol under investigation. The spectra have been shifted for clarity.

$^1, b_0 = 137.5 \pm 0.1\text{ MPa}$ ,  $b_1 = (6.19 \pm 0.02) \cdot 10^{-3}\text{ C}^{-1}$ , and  $C = 0.0894$  are constants taken from Ref. [15]. It should be noted that the temperature and pressure dependence of  $V_s$  was determined experimentally up to  $200\text{ MPa}$  (under the given  $T$  and  $p$  conditions). Hence to obtain  $V_s(T, p)$  at much higher pressures, corresponding to those where FTIR spectra were collected, we calculated them from the Tait equation of state (Eq. (1)). Thus, by combining the isothermal and isobaric FTIR data with the results of volumetric measurements modeled using the Tait formula, the correlation between the  $V_s$ s and the O—H peak positions for any conditions of  $T$  and  $p$  were estimated. IR spectra measured at isochoric point ( $V_s = 0.88\text{ cm}^3\cdot\text{g}^{-1}$ ) are shown in Figure 2(b). To monitor the evolution of the O—H band at isochronal conditions ( $\tau_\alpha = \text{const}$ ), we used dielectric data reported in Ref. [28]. In this paper, a pressure evolution of the glass transition temperature ( $T_g$ ) was evaluated (please see Figure S3). Taking into account that vitrification occurs at constant structural relaxation times (usually, it is defined as temperature or pressure at which  $\tau_\alpha = 100\text{ s}$ ), one can easily determine isochrones along various thermodynamic conditions. Herein, it should be noted that the pressure evolution of the  $T_g$  for the studied alcohol was obtained up to  $1570\text{ MPa}$ . Hence, to evaluate  $T_g$  vs  $p_g$  variation at much higher pressures, comparable to those applied during FTIR experiments, this dependency was further modeled by the well-known empirical Anderson–Anderson formula (see Figure S3 in the SM file) [34]. Having all these analyses done, one can follow the shift of the O—H peak



position under the isobaric, isochoric, and isochronal conditions in **Figure 2**. At first sight, it is visible that there is a red shift of the  $\nu_{\text{O-H}}$  band, the blue-shift one, and the non-monotonic change of this band frequency for isobaric, isochoric, and isochronal conditions, respectively. Nevertheless, to explore these spectral changes in detail, the determined O—H peak positions along different isolines were plotted vs  $p$  and  $T$  in **Figure 3**.

Examination of the plots presented in **Figure 3** revealed: (a) the red shift of the  $\nu_{\text{O-H}}$  band frequency from  $3329 \text{ cm}^{-1}$  (460 MPa) to  $3189 \text{ cm}^{-1}$  (6130 MPa) during isothermal compression at 323 K; (b) the reduction of the  $\nu_{\text{O-H}}$  band frequency from  $3331 \text{ cm}^{-1}$  (293 K) to  $3269 \text{ cm}^{-1}$  (123 K) during cooling at ambient pressure; (c) the blue-shift of the  $\nu_{\text{O-H}}$  band frequency from  $3231 \text{ cm}^{-1}$  (293 K; 2110 MPa) to  $3268 \text{ cm}^{-1}$  (348 K, 2350 MPa) with an increase of temperature at constant specific volume ( $V_s = 0.88 \text{ cm}^3 \cdot \text{g}^{-1}$ ); and (d) a drastic decrease in the  $\nu_{\text{O-H}}$  band frequency from  $3277$  to  $3214 \text{ cm}^{-1}$  along  $T_g(p_g)$  line from  $T = 143 \text{ K}$  to  $T = 293 \text{ K}$ , then the non-monotonically rise of this parameter up to 348 K ( $3241 \text{ cm}^{-1}$ ). It was also observed that for higher specific volume ( $V_s = 1.00 \text{ cm}^3 \cdot \text{g}^{-1}$ ), a smaller change in the O—H peak position for 293 K and 348 K ( $\Delta\nu \sim 27 \text{ cm}^{-1}$ ) occurs than for the lower  $V_s$ : 0.80 and  $0.88 \text{ cm}^3 \cdot \text{g}^{-1}$  ( $\Delta\nu \sim 36 \text{ cm}^{-1}$ ). This observation may suggest that for the higher compression, the temperature fluctuations become more important in controlling the strength of HBs.

However, to quantify this observation, as a final point of our discussion, we analyzed the pressure dependence of the ratio of the isochoric and isobaric activation energies,  $E_V/E_p$  (where  $E_V = R\partial\log(x)/\partial(1/T)|_V$ ,  $E_p = R\partial\log(x)/\partial(1/T)|_p$ ), which is a fundamental tool to verify whether the temperature or density fluctuations govern the  $x$

parameter, which refers to the dynamics. Herein, it should be noted that this kind of analysis was commonly adopted to determine the influence of thermal and molecular packing on the structural and segmental dynamics in low- and high-molecular-weight liquids [9]. Briefly, one can stress that as this ratio equals 0 or 1, the mobility is governed solely either by volume or temperature, respectively. The schematic representation of the discussed scenarios is presented in **Figure 4(a)** for the  $\nu_{\text{O-H}}$  band. The blue arrow depicts the situation, in which the volume controls the shift of  $\nu_{\text{O-H}}$  band. In this case, the change in the temperature at isochoric conditions does not affect the  $\nu_{\text{O-H}}$  position. Consequently, one can observe the horizontal  $\nu_{\text{O-H}}(1/T)$  dependence, ( $E_V/E_p = 0$ ). Contrary, the red arrow reflects the scenario, in which exclusively the temperature controls HBs dynamics. In this situation, the isochronal  $\nu_{\text{O-H}}(1/T)$  overlaps the isobaric one ( $E_V/E_p = 1$ ). Hence, to find out which scenario prevails, we plotted the pressure dependencies of the  $\nu_{\text{O-H}}$  band position at four different isotherms and described them by the exponential functions (see solid lines in **Figure 4(b)**). This procedure allowed us to estimate  $\nu_{\text{O-H}}$  at any pressure at  $T = 293, 308, 323,$  and  $348 \text{ K}$ . Subsequently, employing the equation of state, we predicted the evolution of pressure, when temperature increases at  $V = \text{const}$ . Hence, it was possible to estimate the position of the O—H band along the isochore. We performed these computations starting with a density corresponding to the point measured at  $T = 293 \text{ K}$  and  $p = 0.1 \text{ MPa}$ , see **Figure 4(a)**. Interestingly, the obtained isochoric dependency of the  $\nu_{\text{O-H}}$  band almost perfectly overlaps the experimental points measured at ambient pressure (isobar  $p = 0.1 \text{ MPa}$ ). It means the  $E_V/E_p$  ratio should be close to the unity. In fact, the calculated  $E_V/E_p$  equals 0.97. From this analysis, it becomes clear that temperature is the main

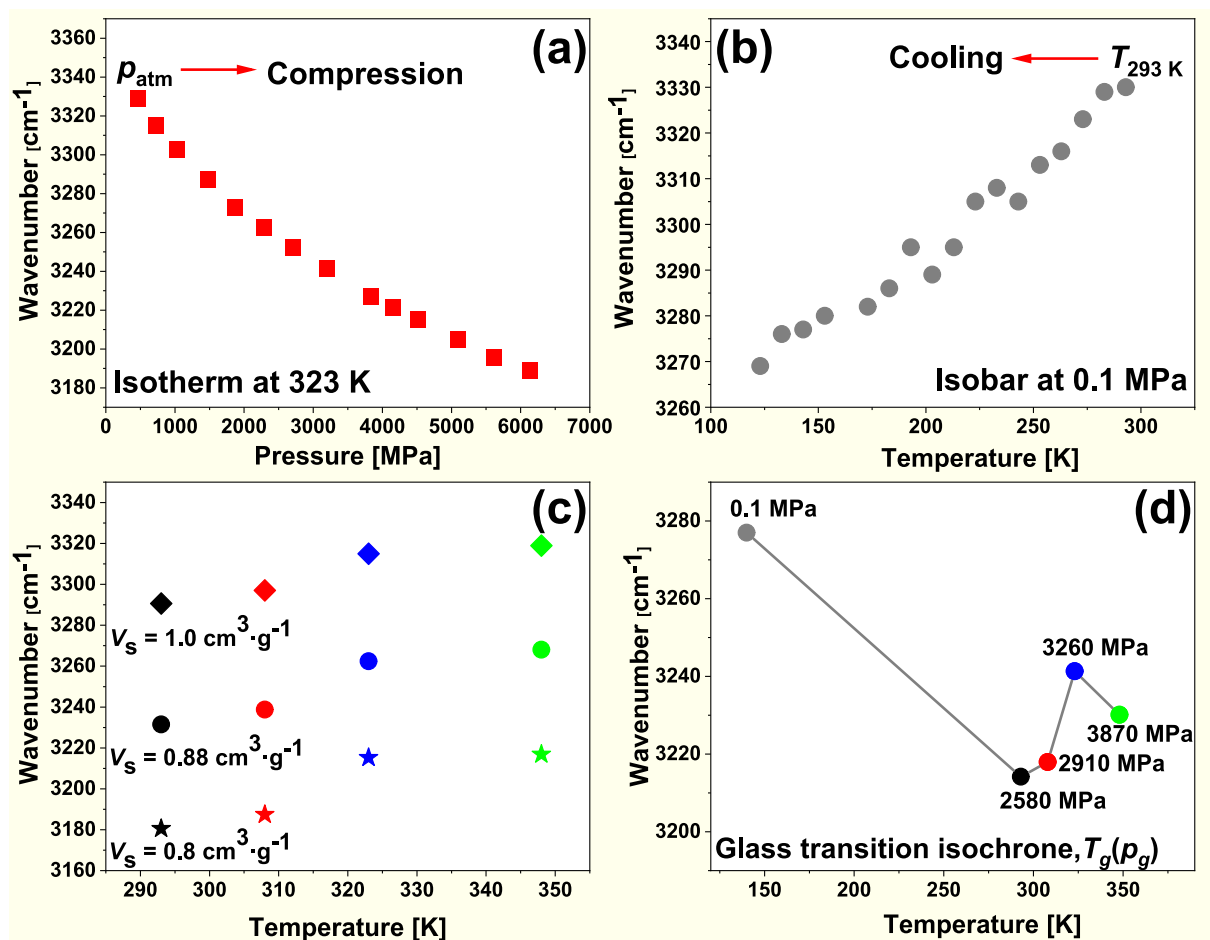


**Fig. 3.** The variation of the O—H band frequency along a) isotherm at 323 K, b) isobar at 0.1 MPa, c) isochore at  $V_s = 0.8, 0.88$  and  $1.0 \text{ cm}^3 \cdot \text{g}^{-1}$ , and d) isochrone ( $\tau_\alpha = 100 \text{ s}$ ) along  $T_g(p_g)$ .

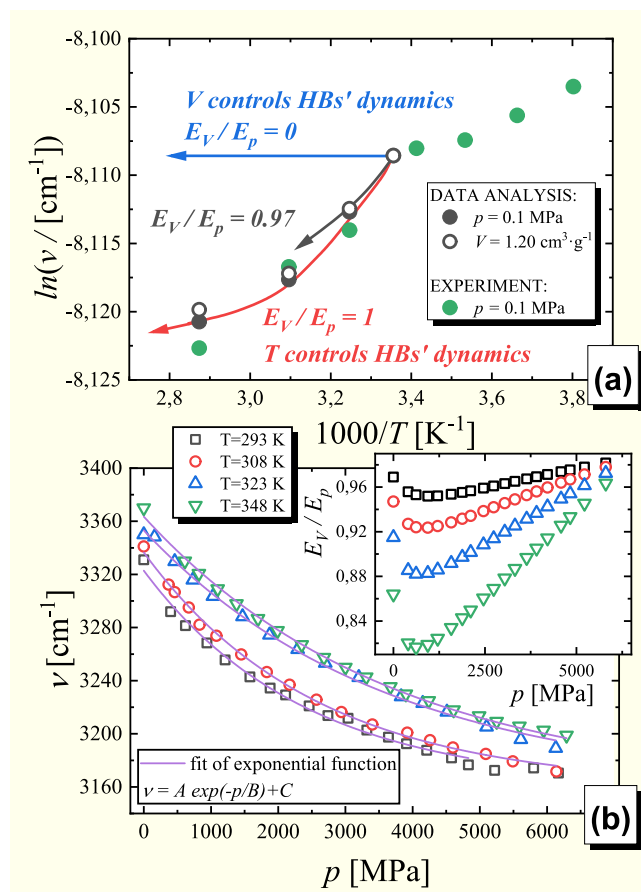


**Fig. 4.** Panel (a) depicts an evolution of the logarithm of the O–H band frequency ( $\nu$ ) as a function of the inverse temperature ( $1000/T$ ). Arrows schematically present the behavior of O–H band frequencies corresponding to the situations in which the dynamics of HBs is governed by the volume (blue arrow,  $E_V/E_p = 0$ ), and the temperature (red arrow,  $E_V/E_p = 1$ ). The black arrow illustrates the results of our calculations. Panel (b) presents O–H band frequencies ( $\nu$ ) as a function of  $p$ . The pressure dependence of  $E_V/E_p$  is shown in the inset of panel (b).

parameter controlling the intermolecular hydrogen bonds that influence the intramolecular dynamics of O–H moieties.

Further deeper analysis of the data revealed that the  $E_V/E_p$  parameter changes non-monotonically with the pressure for all isotherms up to the values close to the unity (from 0.86 to 0.97 at 0.1 MPa to 0.96–0.98 at 5800 MPa). Moreover, the characteristic minimum occurs at ca. 600 MPa. Interestingly, such pressure corresponds to the upper limit of  $p$ , for which the TS rule for 2E1H is obeyed [13]. One can add that below and above this  $p$ , one can scale the relaxation times measured at different thermodynamic conditions with constant and  $\tau_\alpha$ -dependent scaling exponent [13], respectively. What is more, the  $E_V/E_p$  approaches unity with the compression (see the inset in Figure 4(b)). It means that temperature plays a dominant role in controlling the intramolecular dynamics of O–H units. Moreover, panel (b) in Figure 4 revealed that as the temperature of the isotherm increases, the  $E_V/E_p$  decreases, suggesting the increasing role of density. The other interesting result is that the weaker HBs (the higher values of the O–H band frequency) are more sensitive to changes in the volume than the stronger HBs. Finally, it should be noted that the obtained values of  $E_V/E_p$  ratio are close to those determined from dielectric measurements for the Debye relaxation ( $E_V/E_p = 0.76$ ), which is regarded as a manifestation of the dynamics of HBs [15]. Therefore, the analysis of the O–H stretch band position at high  $p$  clearly indicates that there is a close correlation between the dynamics of the Debye relaxation observed in dielectric loss spectra and

the intramolecular dynamics of O–H units or the strength of HBs. What is more, the value of  $E_V/E_p$  obtained herein is also comparable to those estimated for the structural relaxation in other H-bonded liquids with more than one hydroxyl group, e.g., glycerol ( $E_V/E_p = 0.97$ ), sorbitol ( $E_V/E_p = 0.87$ ), glycol derivatives (propylene glycol:  $E_V/E_p = 0.88$ , dipropylene glycol:  $E_V/E_p = 0.86$ , and tripropylene glycol:  $E_V/E_p = 0.83$ ) [15]. Herein it should be noted that the value of this parameter for the non-associated materials, such as *ortho*-terphenyl ( $E_V/E_p = 0.55$ ), salol ( $E_V/E_p = 0.43$ ), propylene carbonate ( $E_V/E_p = 0.64$ ), and phenylphthalindimethylether ( $E_V/E_p = 0.53$ ) is much lower [15]. These simple examples indicate that so high values of  $E_V/E_p$  for liquids associating via HBs are connected to the intramolecular dynamics of O–H units.

#### 4. Conclusions

In this paper, we considered a fundamental question from the perspective of physics, chemistry, and biology: which parameter does determine the properties of HBs - temperature or density (at given thermodynamic conditions)? For this purpose, we have analyzed the variation of the strength of HBs in 2E1H, directly through the shift of the O–H band position in the FTIR spectra, upon  $T$  and  $p$  variation. Then, the obtained FTIR results were combined with the dielectric and volumetric data. In this way, we were able to describe the temperature and pressure dependence of H-bonding energy along various isolines. What is more, we calculated the  $E_V/E_p$  parameter, which provides a direct insight into the impact of density and temperature on the dynamics of an associating system. Adopting this kind of analysis for the O–H band frequencies of simple alcohol – 2E1H allowed us to demonstrate that  $T$  controls the intermolecular HBs affecting the intramolecular dynamics of O–H moieties. However, it must be added that the impact of density grows together with increasing  $T$  and weakening of H-bonding interactions. It was also found that the temperature plays a dominant role in the case of stronger HBs, while for the weaker ones, the density effect on the association process via HBs gets stronger. Thus, the presented studies enable unprecedented insight into the behavior of HBs and the dynamics of associating liquids. What is more, they open completely new pathways to explore HBs in various kinds of materials and an even better understanding of these fundamental electrostatic interactions.

#### CRediT authorship contribution statement

**Barbara Hachula:** Writing – original draft, Writing – review & editing, Investigation, Formal analysis, Visualization, Methodology, Conceptualization. **Ewa Kamińska:** Writing – original draft. **Kajetan Koperwas:** Formal analysis. **Roman Wrzalik:** Formal analysis. **Karolina Jurkiewicz:** Visualization. **Magdalena Tarnacka:** Investigation. **Demetrio Scelta:** Investigation. **Samuele Fanetti:** Investigation. **Sebastian Pawlus:** Investigation, Funding acquisition. **Marian Paluch:** Supervision. **Kamil Kamiński:** Conceptualization, Supervision.

#### Declaration of Competing Interest

The authors declare that they have no known competing financial interests or personal relationships that could have appeared to influence the work reported in this paper.

#### Data availability

Data will be made available on request.

#### Acknowledgment

The research leading to these results has received funding from LASERLABEUROPE (Grant agreement No. 654148, European Union's

Horizon 2020 research and innovation programme; Proposal No. LENS002738). B.H, K.J., K.K., and S.P. are thankful for the Polish National Science Centre's financial support within the OPUS project (Dec. no UMO-2019/35/B/ST3/02670).

## Appendix A. Supplementary material

Supplementary data to this article can be found online at <https://doi.org/10.1016/j.saa.2022.121726>.

## References

- [1] S. Fanetti, M. Citroni, K. Dziubek, M.M. Nobrega, R. Bini, The role of H-bond in the high-pressure chemistry of model molecules, *J. Phys. Condens. Matter* 30 (9) (2018) 094001, <https://doi.org/10.1088/1361-648X/aaa8cf>.
- [2] S.K. Sikka, S.M. Sharma, The hydrogen bond under pressure, *Phase. Transit.* 81 (10) (2008) 907–934, <https://doi.org/10.1080/01411590802098864>.
- [3] G. Nielsen, H. Schwalbe, Hydrogen bonds under pressure, *Nat. Chem.* 4 (9) (2012) 693–695, <https://doi.org/10.1038/nchem.1443>.
- [4] M. Citroni, M. Ceppatelli, R. Bini, V. Schettino, Laser-Induced Selectivity for Dimerization Versus Polymerization of Butadiene Under Pressure, *Science* 295 (5562) (2002) 2058–2060.
- [5] D. Chelazzi, M. Ceppatelli, M. Santoro, R. Bini, V. Schettino, High-pressure synthesis of crystalline polyethylene using optical catalysis, *Nat. Mater.* 3 (7) (2004) 470–475, <https://doi.org/10.1038/nmat1147>.
- [6] P.F. McMillan, New materials from high-pressure experiments, *Nat. Mat.* 1 (1) (2002) 19–25, <https://doi.org/10.1038/nmat716>.
- [7] L. Zhang, Y. Wang, J. Lv, Y. Ma, Materials discovery at high pressures, *Nat. Rev. Mater.* 2 (2017) 17005, <https://doi.org/10.1038/natrevmats.2017.5>.
- [8] C. Buzea, K. Robbie, Assembling the puzzle of superconducting elements: a review, *Supercond. Sci. Technol.* 18 (1) (2005) R1–R8, <https://doi.org/10.1088/0953-2048/18/1/R01>.
- [9] G. Floudas, M. Paluch, A. Grzybowski, K. Ngai, *Molecular dynamics of glass-forming systems: Effects of pressure*, Springer-Verlag, Berlin, Heidelberg, 2011.
- [10] C.M. Roland, M. Paluch, T. Pakula, R. Casalini, Volume and temperature as control parameters for the dielectric relaxation of polymers and molecular glass formers, *J. Phil. Mag.* 84 (2004) 1573–1581, <https://doi.org/10.1080/14786430310001644350>.
- [11] T. Atake, C.A. Angell, Pressure dependence of the glass transition temperature in molecular liquids and plastic crystals, *J. Phys. Chem.* 83 (25) (1979) 3218–3223, <https://doi.org/10.1021/j100488a007>.
- [12] H. S. Ashbaugh, Response to “Comment on ‘A simple molecular thermodynamic theory of hydrophobic hydration’” [*J. Chem. Phys.* 119 (2003) 10448]. *J. Chem. Phys.* 119 (2003) 10450, <https://doi.org/10.1063/1.1619938>.
- [13] S. Pawlus, M. Paluch, A. Grzybowski, Communication: Thermodynamic scaling of the Debye process in primary alcohols, *J. Chem. Phys.* 134 (4) (2011) 041103, <https://doi.org/10.1063/1.3540636>.
- [14] A. Reiser, G. Kasper, C. Gainaru, R. Böhmer, Communications: High-pressure dielectric scaling study of a monohydroxy alcohol, *J. Chem. Phys.* 132 (18) (2010) 181101, <https://doi.org/10.1063/1.3421555>.
- [15] D. Fragiadakis, C.M. Roland, R. Casalini, Insights on the origin of the Debye process in monoalcohols from dielectric spectroscopy under extreme pressure conditions, *J. Chem. Phys.* 132 (14) (2010) 144505, <https://doi.org/10.1063/1.3374820>.
- [16] C.M. Roland, S. Hensel-Bielowka, M. Paluch, R. Casalini, Supercooled dynamics of glass-forming liquids and polymers under hydrostatic pressure, *Rep. Prog. Phys.* 68 (6) (2005) 1405–1478, <https://doi.org/10.1088/0034-4885/68/6/R03>.
- [17] K.L. Ngai, S. Capaccioli, Impact of the application of pressure on the fundamental understanding of glass transition, *J. Phys.: Condens. Matter* 20 (24) (2008) 244101, <https://doi.org/10.1088/0953-8984/20/24/244101>.
- [18] C.M. Roland, R. Casalini, M. Paluch, Isochronal temperature–pressure superpositioning of the  $\alpha$ -relaxation in type-A glass formers, *Chem. Phys. Lett.* 367 (2003) 259–264, [https://doi.org/10.1016/S0009-2614\(02\)01655-X](https://doi.org/10.1016/S0009-2614(02)01655-X).
- [19] W.L. Jorgensen, M. Ibrahim, Pressure dependence of hydrogen bonding in liquid methanol, *J. Am. Chem. Soc.* (1982) 373–378, <https://doi.org/10.1021/ja00366a001>.
- [20] L.J. Root, B.J. Berne, Effect of pressure on hydrogen bonding in glycerol: A molecular dynamics investigation, *J. Chem. Phys.* 107 (11) (1997) 4350–4357, <https://doi.org/10.1063/1.474776>.
- [21] A. Arencibia, M. Taravillo, F.J. Perez, J. Nunez, V.G. Baonza, Effect of pressure on hydrogen bonding in liquid methanol, *Phys. Rev. Lett.* 89 (2002), 195504, <https://doi.org/10.1103/PhysRevLett.89.195504>.
- [22] J.F. Mammone, S.K. Sharma, M. Nicol, Raman spectra of methanol and ethanol at pressures up to 100 Kbar, *J. Phys. Chem.* 84 (23) (1980) 3130–3134, <https://doi.org/10.1021/j100460a032>.
- [23] P. Griffiths, J. A. de Hasseth, *Fourier Transform Infrared Spectrometry* (2nd ed.), Wiley-Blackwell, 2007.
- [24] P.A. Guńka, A. Olejniczak, S. Fanetti, R. Bini, I.E. Collings, V. Svitlyk, K.F. Dziubek, Crystal structure and non-hydrostatic stress-induced phase transition of urotropine under high pressure, *Chem. Eur. J.* 27 (3) (2021) 1094–1102, <https://doi.org/10.1002/chem.202003928>.
- [25] W. Dzwolak, M. Kato, Y. Taniguchi, *Fourier transform infrared spectroscopy in high-pressure studies on proteins*, *Biochim. et Biophys. Acta (BBA) - Protein Struct. Mol. Enzymol.* 1595 (1–2) (2002) 131–144.
- [26] R. Bini, R. Ballerini, G. Pratesi, H.J. Jodl, Experimental setup for Fourier transform infrared spectroscopy studies in condensed matter at high pressure and low temperatures, *J. Rev. Sci. Instrum.* 68 (8) (1997) 3154–3160, <https://doi.org/10.1063/1.1148261>.
- [27] M. Wojdyr, Fityk: a general-purpose peak fitting program, *J. Appl. Cryst.* 43 (5) (2010) 1126–1128, <https://doi.org/10.1107/S0021889810030499>.
- [28] S. Pawlus, M. Paluch, M. Dzida, Molecular dynamics changes induced by hydrostatic pressure in a supercooled primary alcohol, *J. Phys. Chem. Lett.* 1 (21) (2010) 3249–3253, <https://doi.org/10.1021/jz101288v>.
- [29] G.A. Jeffrey, *An Introduction to Hydrogen Bonding*, Oxford University Press, 1997.
- [30] D. Li, Z. Zhang, W. Jiang, Y.u. Zhu, Y.i. Gao, Z. Wang, Uncooperative effect of hydrogen bond on water dimer, *Chin. Phys. Lett.* 38 (1) (2021) 013101, <https://doi.org/10.1088/0256-307X/38/1/013101>.
- [31] J.C. Howard, J.L. Gray, A.J. Hardwick, L.T. Nguyen, G.S. Tschumper, Getting down to the fundamentals of hydrogen bonding: Anharmonic vibrational frequencies of (HF)<sub>2</sub> and (H<sub>2</sub>O)<sub>2</sub> from ab initio electronic structure computations, *J. Chem. Theory Comput.* 10 (12) (2014) 5426–5435, <https://doi.org/10.1021/ct500860v>.
- [32] J.R. Lane, CCSDTQ optimized geometry of water dimer, *J. Chem. Theory Comput.* 9 (1) (2013) 316–323, <https://doi.org/10.1021/ct300832f>.
- [33] Y. Song, in: *Applications of Molecular Spectroscopy to Current Research in the Chemical and Biological Sciences*, InTech, 2016, <https://doi.org/10.5772/64617>.
- [34] M. Tarnacka, W.K. Kipnusu, E. Kaminska, S. Pawlus, K. Kaminski, M. Paluch, The peculiar behavior of the molecular dynamics of a glass-forming liquid confined in native porous materials – the role of negative pressure, *Phys. Chem. Chem. Phys.* 18 (34) (2016) 23709–23714, <https://doi.org/10.1039/C6CP03923E>.